www.amlett.com, www.vbripress.com/aml, DOI: 10.5185/amlett.2016.6156 Published online by the VBRI Press in 2016

Influence of anodization parameters on morphology of TiO_2 nanostructured surfaces

Mukta Kulkarni[1,#], Anca Mazare[2,#], Patrik Schmuki[2], Ales Iglic[1*]

[1]*Laboratory of Biophysics, Faculty of Electrical Engineering, University of Ljubljana, Ljubljana SI-1000, Slovenia*
[2]*Department of Materials Science and Engineering, University of Erlangen–Nuremberg, Erlangen, Germany*
[#]*Equally share the first authorship*

[*]Corresponding author. Tel: (+386) 14-768825; E-mail: ales.iglic@fe.uni-lj.si

Received: 11 September 2015, Revised: 18 November 2015 and Accepted: 05 December 2015

ABSTRACT

Titanium (Ti) is one of the most promising biomaterial for biomedical devices due to its high corrosion resistance and specific combination of strength and biocompatibility. Titanium dioxide (TiO_2) nanostructures are obtained by electrochemical anodization of Ti foils under self-organization condition; anodization parameters such as anodization time, voltage, temperature and most important electrolyte composition are critical for the resulting morphology. Nanostructures are grown in ethylene glycol (EG) based electrolytes and we evaluated the influence of the water content, as no nanostructures are formed in the electrolyte without water addition, and with increasing water content, either nanopores or nanotubes are obtained (depending also on the applied potential and anodization time). The increase in water content in the electrolyte enables the slow transition from nanopores to nanotubes, which occurs by a pore-wall splitting mechanism. From the current results, one can conclude that the water in the electrolyte has a definite effect on the type of nanostructures obtained by electrochemical anodization in organic electrolytes. This current investigation of effect of water in EG based electrolytes is useful for obtaining the desired morphology of the nanostructures (diameter, length, open-top morphology) for specific bioapplications.

Keywords: Electrochemical anodization; TiO_2 nanostructured surfaces; topography; bioapplications.

Introduction

Titanium and titanium alloys are of high interest in various applications **[1-5]** more specifically for biomedical applications, due to their excellent mechanical properties, high corrosion resistance and good biocompatibility **[1-3]**. To improve stability of such implant materials, to enhance cell response and to inhibit detrimental phenomena, the surface of implants is usually modified with various coatings, thermal procedures or surface treatments at the micro and nano level. Nowadays, for biomaterials, the focus is on the nano level, i.e. nanostructuring of the surface (increasing surface area, enhancing biocompatibility, etc.) and from the pletoria of available nanostructuring techniques, nanostructures can be easily grown by electrochemical anodization. Although the first report on anodization of Ti in 1984 (by Assefpour-Dezfuly *et al.* **[6]**) was overlooked, such structures were later reported only in 1999 by Zwilling *et al.* **[7, 8]** and following, other methods were also reported on obtaining TiO_2 nanotubes, methods such as hydrothermal process **[9]**, sol-gel **[10]** or template **[11]**.

The advantages of electrochemical anodization lie in the ease of application and control of the nanostroctures' morphology while ensuring that the coating is directly on the biomaterial's surface **[12, 13]**. Nanostructures can be grown under self-organizing conditions on titanium or its alloys, by anodizing in fluoride containing electrolytes (reports also indicate growth of nanotubes in fluoride-free electrolyte, however the control over the morphology is limited **[14]**). Generally, the anodization electrolytes contain hydrofluoric acid (HF) or fluoride salts in an aqueous acidic solution (generation I **[15, 16]**), in basic salts (generation II **[17]**) or in organic electrolytes with small additions of water (generation III **[18]**). Currently, the most frequently used electrolytes are organic and are based on glycerol or EG **[18, 19]**, and this is due to the fact that such organic electrolytes lead to much higher aspect ratio (higher surface are) and more uniform growth with a hexagonal ordering **[13]**.

As a part of the continuing endeavor to utilize titanium dioxide (TiO_2) nanostructures in the development of biomedical devices, the effects of various anodization conditions (time, voltage and water content in the electrolyte) on the formation of nanostubular structures on both titanium **[19]** and titanium alloys **[20-24]** was further investigated. The morphology and dimensions of TiO_2 nanotubes play a critical roles in determining their performance in various biomedical applications. That is, the efficiency of many TiO_2 biomedical devices depends on the geometry and surface area of the nanostructured TiO_2 layers, therefore the self-organized anodic growth of TiO_2 nanotubes has attracted significant interest **[13, 25]**. In this respect, the nanotube diameter and length determine the aspect ratio of these structures and influence the sensitivity and selectivity of nanoscale devices. Consequently, the ability to control these parameters by modifying the anodization conditions is imperative for new

developements in various fields. Additionaly, in the field of biomimetic materials and tissue implant technology, the importance of nanometric scale surface topography and roughness of biomaterials is, besides chemical surface modifications, increasingly becoming recognized as a crucial factor for tissue acceptance and cell survival **[26-28]**. For example, it is known that the diameter size is the key factor dictating in the interactions with cells (mesenchymal stem cells, endothelial cells, osteoblasts, osteoclasts, etc.) and 15 nm diameter nanotubes enhance cell adhesion, proliferation and differentionation compared to 100 nm diameter nanotubes, which lead to cell apoptosis **[29-32]**. Moreover, it is worth mentioning that in all cases small diameter nanotubes improved cell interactions as compared to the non-nanostructured substrates (either untreated foil or a 50 nm thick TiO_2 compact layer). Previous studies have also shown that surface modification of Ti significantly changed bacterial responses **[33]** and can influence interactions with macrophage cells (especially as biomaterial implantantion is often limited by macrophage-related inflammation) **[34-36]**.

Besides, nanostructured TiO_2 can be used as a platform for various biomolecules coating/loading or growth factor immobilization **[30, 37]**, Ag nanoparticle decoration **[38, 39]** or other nanoparticles showing either antibacterial effects or increasing osseointegration **[38, 39]**. As-formed TiO_2 nanotubes grown by anodization are usually amorphous but depending on the anodization conditions (temperature, time or how high is the voltage) low crystallinity is observed (anatase phase). Crystallinity (anatase, anatase and rutile mixture) is induced by annealing, and showed also promising properties in terms of biocompatibility **[21, 40, 41]**.

The present study aims towards an understanding of the role of anodization parameters such as time, voltage and water content in EG based electrolytes in the synthesis of arrays of TiO_2 nanostructures and in their corresponding morphologies. The purpose of optimizing the anodizaton parameters is to tailor the morphology of nanotubes to a spefific diameter size and length, which leads to an increased biocompatibility and outstanding cellular interactions. The nanotopography of TiO_2 has a significant influence on the adherence and the cell behavior in biomedical applications. Though the influence of the water content in organic based electrolytes was previously investigated **[42, 43]**, the present paper mainly focuses on the influence of anodization parameters in EG based electrolytes on the morphology of nanostructures with emphasis also on obtaining small diameter (15 nm) nanostructures. The current investigation of the effect of the water contact in electrolyte and other anodization parameters on the morphology of nanostructures is useful for a better tailoring of the desired morphology of the nanostructures (nanopores or nanotubes) TiO_2 surfaces for bioapplications.

Experimental

Materials

Ti-foils of 0.1 mm thickness (99.6 % purity) were obtained from Advent Research Materials, England. The distilled water used during the entire study was purified by Werner–Reverse osmosis equipment. Hydrofluoric acid (HF) and the solvents, namely Ethylene Glycol (EG), ethanol, and acetone, were purchased from Sigma–Aldrich, Germany and used without further purification.

Experimental

Various TiO_2 nanostructures were fabricated by electrochemical anodization. Prior to anodization, titanium foils were degreased by successive ultrasonication in acetone, ethanol and deionized (DI) water for 5 min each and dried in nitrogen stream. For anodization experiments, EG based electrolyte was used which contains varying amounts of water but with same concentration of HF. All the anodization experiments were carried out at room temperature (~20 ^{o}C) in a two-electrode system with a titanium foil as the working electrode and platinum gauze as the counter electrode. Experimental parameters such as anodization voltage, time and composition of electrolyte were varied and their effect was observed on diameters and lengths of obtained TiO_2 nanostructures. As-formed nanostructures were kept in ethanol for 2 hours as to remove all organic components from the electrolyte, washed with distilled water and dried in a nitrogen stream.

Characterization

The morphology of the as-formed TiO_2 nanostructured surfaces was observed using a field-emission scanning electron microscope – Hitachi FE-SEM S4800. Mechanically cracked samples were used to obtain cross-section images. The chemical composition of as-formed nanostructures was investigated by X-ray photoelectron spectroscopy (XPS) (PHI 5600, spectrometer, USA) using AlKα monochromatized radiation and peaks were calibrated to C1s peak at 284.8 eV. The crystallinity of the TiO_2 nanostructures was evaluated by X-ray diffraction (XRD) patterns using a X'pert PhilipsMPD with a Panalytical X'cel-erator detector, Germany (graphite mono-chromized Cu Kα radiation, wavelength of 1.54056 Å).

Results and discussion

In the following sections, the influence of different anodization parameters on the morphology of nanostructrures (diameter, length, and the type of obtained nanostructure – nanopores or nanotubes) as well as their chemical composition and crystallinity are evaluated. It is well known that the morphology of TiO_2 nanotubes can be easily tailored to specific diameter size or length **[13]**; nevertheless, to establish a good control ensuring all the desired morphological characteristics as well as an open top morphology (no initiation layer or nanograss formation) an anodization parameters screening is helpful.

Influence of applied voltage on the diameter and length of the nanostructures

First of all, the influence of the applied voltage on the growth and morphology of the nanostructures was evaluated for EG based electrolyte containing 8 M water and 0.2 M HF. At the same time, we also evaluated similar aspects using a 6 M water content electrolyte.

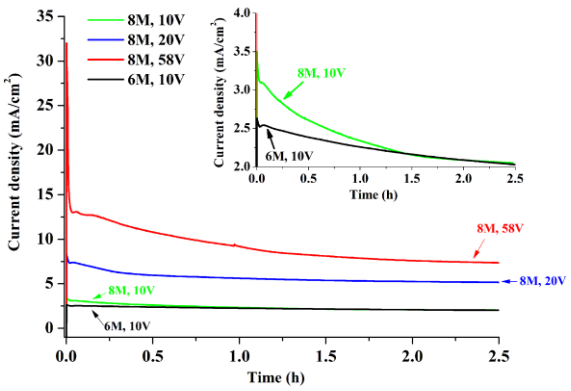

Fig. 1. Current profiles for nanostructrures obtained in EG based electrolytes (8 M water content) at different anodization potential (10, 20 or 58 V) for an anodization time of 2.5 h. A current profile for nanostructures grown in 6 M water content at 10 V for 2.5 h is also shown for comparison.

Fig. 1 presents the current profiles (I-t curves) for selected samples, for an anodization time of 2.5 h in 8 M (10, 20 and 58 V) and in 6 M (10 V). It is evident that the I-t plots present typical curves for a highly organized oxide pore arrangement or nanotube formations, where formation and chemical dissolution of the oxide are in optimum range **[13]**. The typical I-t curve can be divided into three regions, with region I – current decreases exponentially due to the coverage of the surface with an oxide film, region II – a rise in the current due to the surface area increase (as a result of porosification), and region III – steady-state conditions where the oxide is formed continuously at the bottom. In our case, the three regions are observed for all studied nanostructures, even for potentials as low as 10 V (inset in **Fig. 1**). Furthermore, it is clearly evident that higher applied potentials lead to higher current densities, and while a similar trend is observed for the water content inside the electrolyte (comparing the 6 M and 8 M anodization at 10 V) one can see that 8 M has a higher current value in beginning and that, after 1.5 hours of anodization, the same steady-state value of the current, as for 6 M, is reached.

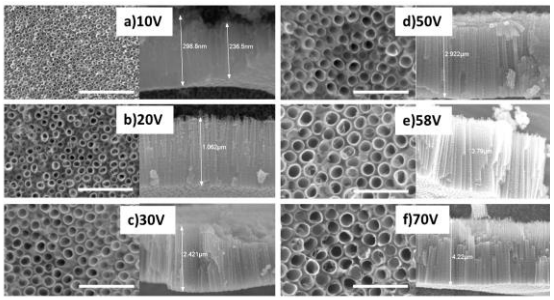

Fig. 2. Top view and cross-section SEM images for nanotubes grown in EG based electrolyte containing 8 M water, anodization time was fixed at 2.5 h (Scale bar is 500 nm), at different anodization potentials of a) 10 V, b) 20 V, c) 30 V, d) 50 V, e) 58 V and f) 70 V.

Fig. 2 presents top-view and cross-section SEM images for nanotubes obtained in EG based electrolyte with 8 M water content and fixed time (2.5 h), emphasizing on the influence of applied potential on the nanotubes' diameter and length. From the top view images, it is evident that diameters of nanotubes increase with the applied potential (in the range of 10 -70V as shown in **Fig. 2**) and the cross-section images of the nanotubular layer show that the applied voltage has a clear effect also on lengths of nanostructures, increasing with increasing applied potential. To note, that in all cases there is no initiation layer and in these conditions no nanograss formation on the top of the nanostructures, meaning that it is an open-top morphology. The fact that the nanotubes are initiation layer free can be due to the presence of HF in the electrolyte which makes it more acidic and etches much faster the initiation layer (for example, for shorter anodization times of 1.5 h, an initiation layer was also observed), while in NH_4F EG based electrolytes it is difficult to obtain initiation layer free nanotubes **[44]**.

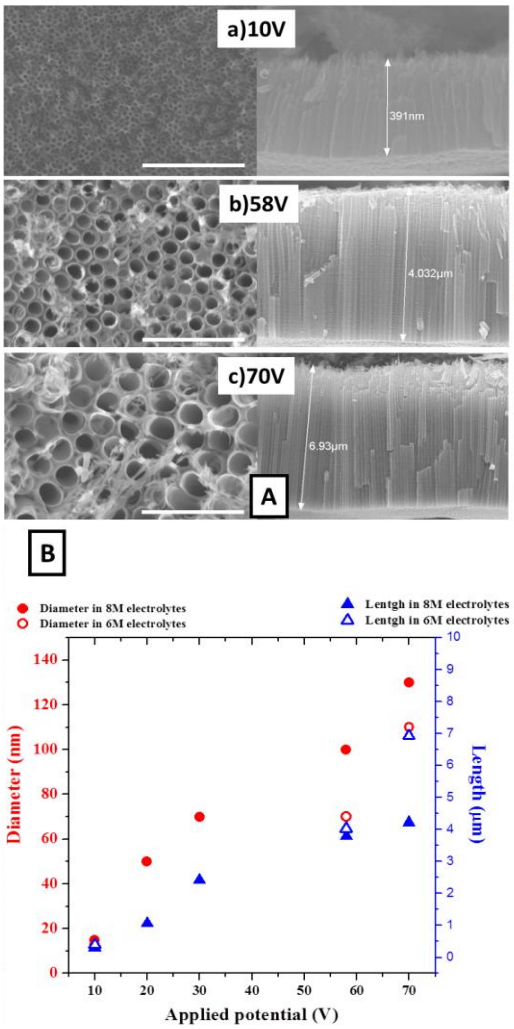

Fig. 3. (A) Top view and cross-section SEM images for selected nanostructures grown in EG based electrolyte containing 6 M water, anodization time was fixed at 2.5 h (Scale bar is 500 nm) (B) Influence of the anodization voltage on the diameter and length of nanotubular structures for EG based electrolyte containing 8 M and 6 M water (anodization time of 2.5 h).

Further, we also evaluated the morphology of nanostructures grown in an EG based electrolyte containing 6 M water and **Fig. 3(A)** presents the top view and cross-section SEM images of selected nanostructures (grown at 10, 58 and 70V). Similar trends were observed as in case of structures obtained in 8 M water. The influence of the

anodization voltage on the diameter and length of nanotubular structures for EG based electrolyte containing 8 M and 6 M water content (anodization time of 2.5 h) is summarized in **Fig. 3(B)**. From **Fig. 3(B)** it can be observed that for both 6 and 8 M water content, the applied potential has a defined effect on the diameter and lengths of nanostructures, significantly increasing with increasing anodization voltage. However, at voltages higher than 80 V for an anodization time of 2.5 h, the nanostructures get etched and nanograss is formed (that is, at the anodization time of 2.5 h, the growth rate of nanotubes at the metal/oxide interface is already smaller than the chemical dissolution occurring at the nanotube top/electrolyte interface); for such high voltages in the range of 80-100 V and using 6 or 8 M water EG electrolytes, shorter anodization times are needed (around 1h) – data not shown.

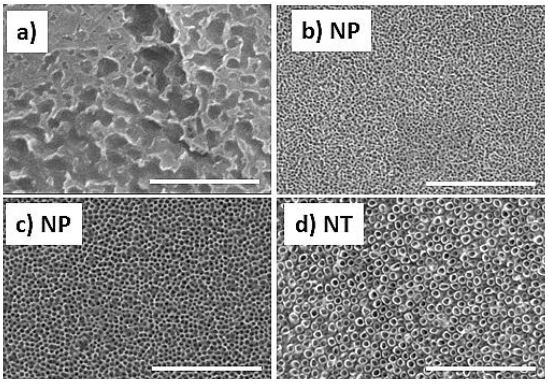

Fig. 4. Influence of water content on the nanostructures' surface, evaluated at a fix applied potential of 10 V and anodization time of 2.5 h for a water content of a) No water, b) 2 M, c) 4 M, and d) 8 M water (Scale bar is 500 nm).

Influence of water content and anodization time on the morphology of TiO_2 nanostructures

It was previously observed that the amount of water inside the electrolyte dictates the obtained morphology of the nanostructures (either nanopores or nanotubes), and nanotube surfaces (NTs) are formed through a pore-wall-splitting mechanism from the nanopores (NPs) structures **[45]**. Nanotube formation is assigned to the selective dissolution of the fluoride rich layer present at the cell boundaries of ordered porous structures formed in fluoride electrolytes **[45]**. The nanopores have a honeycomb like structure with no tube to tube separation, as opposed to nanotubes.

To evaluate this aspect, the anodization voltage and anodization time were fixed to 10 V and 2.5 h respectively, but the electrolyte composition was varied, namely, the water content was varied between no added water, up to a water content of 8 M. The resulting structures are presented in **Fig. 4**, and the key influence of the water content on the morphology of the nanostructures is evident as for the electrolyte with no added water the self-organized anodic growth conditions are not established, while for 2 M and 4 M nanopores are obtained and for 8 M the resulting nanostructure is nanotubular (a water content of 6 M leads to a mixture of both, as in some parts the structure is nanoporous while in others it is nanotubular – these aspects will be further discussed in next section). The lengths of the nanostructures were of 142 nm, 379 nm and 370 nm, respectively with 2 M, 4 M and 8 M water content in the electrolyte. Furthermore, a similar trend was observed for 5 h experiments, where a 2 M water content led still to NPs, while 4 M and 6 M lead to NTs (data not shown). The lengths of nanostructures for 5 h experiments were 324 nm, 350 nm, 495 nm and 590 nm respectively for 2, 4, 6 and 8 M water content in the electrolyte.

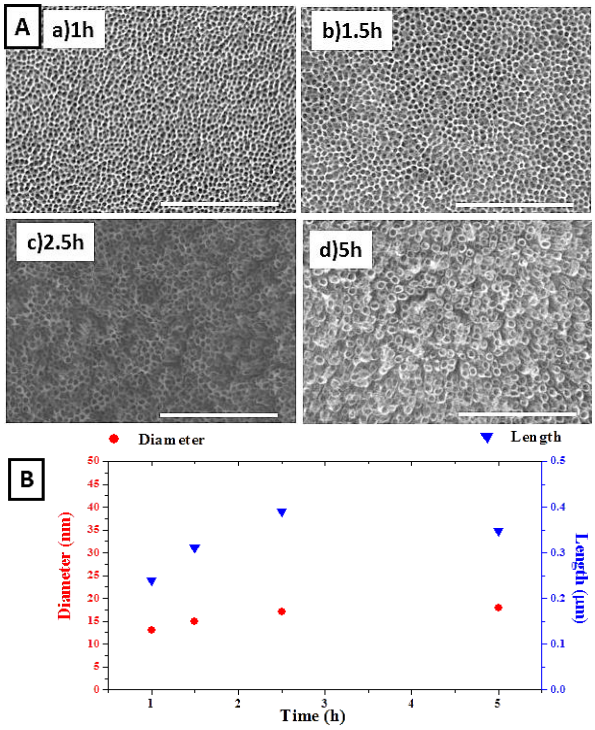

Fig. 5. (A) Top view SEM images of nanostructures obtained at 10 V in a 6 M water content EG based electrolyte (Scale bar is 500 nm), (B) influence of anodization time on morphology of nanostructures grown at 10 V in a 6 M water content EG based electrolyte.

One more key parameter influencing the formation and type of obtained nanostructure is the anodization time. Therefore, we fixed the anodization potential at 10 V, and using a 6 M water content electrolyte, we evaluated the influence of the anodization time on the resulting nanostructure morphology – **Fig. 5** presents the SEM top-view images and an overview of the morphology data. At lower anodization times, nanopores are formed and have small diameters (≈13 nm) and with increasing anodization time, the diameters slightly increase (≈15 nm). With a further increase of the experimental anodization time, the transition from nanopores to nanotubes was observed at 2.5 h and then at even longer anodization time (5 h) the tubes get slightly etched at the top (as seen in **Fig. 2(d)**, there are small remnants on the top of the nanotubes) and the tube wall thickness is further etched resulting in a small increase in the diameter size.

Chemical composition and crystallinity of as-formed TiO_2 nanostructures

To verify the chemical composition and the crystallinity of the different nanostructrures, selected samples were examined by XPS and XRD. For XPS, we evaluated the

following nanostructures: nanopores (obtained in 8 M water content EG based electrolyte, by anodizing at 10 V for 1 h), and nanotubes diameter of 15 nm, 50 nm, and 100 nm - that were all obtained in 8 M water content EG based electrolyte by anodizing for 2.5 h at 10, 20 and 58 V, respectively.

Fig. 6(a) presents the XPS survey patterns with, typical peak signals of Ti (Ti3p at ≈38.4 eV, Ti2p at ≈458.4 eV, Ti2s at ≈565 eV), O (O1s at at ≈530 eV), F (F1s at ≈682 eV), and C (C1s at ≈284.8 eV) – also, a weak N peak signal is observed at ≈402 eV (N1s). The high-resolution scan of the Ti2p **(Fig. 6(b))** with the $Ti2p_{3/2}$ position at 458.4 eV indicates the Ti^{4+} state in the TiO_2. The O1s peak at 530 eV confirms this. Furthermore, due to the presence of the fluoride in the electrolyte, F1s is also present in the sample (see F1s peak at 684 eV, in **Fig 6(c)**).

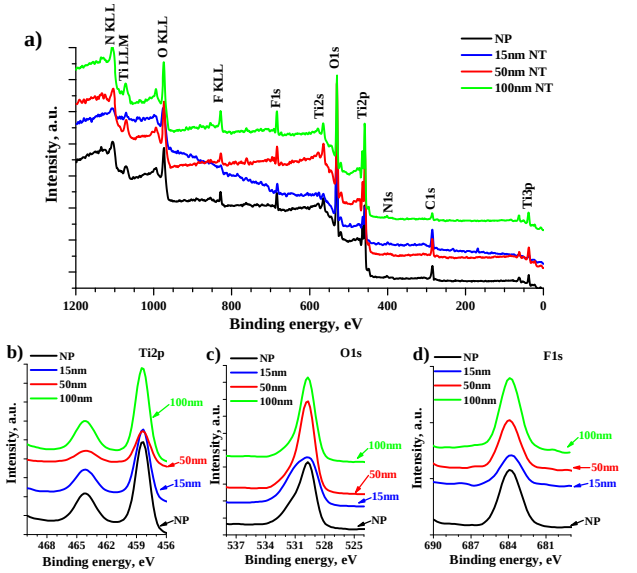

Fig. 6. XPS characterization of the selected nanostructures, nanopores and different diameter (15, 50 or 100 nm) nanotubes: a) survey patterns and high-resolution scans for c) Ti2p, c) O1s and d) F1s.

Table 1. Atomic percent (%) composition determined from XPS measurements.

Sample	C at.%	N at.%	O at.%	F at.%	Ti at.%	F/Ti ratio
nanopores	23.30	1.78	49.06	7.63	18.23	0.42
15 nm	34.42	2.50	49.50	3.94	9.64	0.41
50 nm	23.24	1.07	52.93	7.48	19.69	0.38
100 nm	10.99	1.29	54.95	9.33	23.43	0.39

Table 1 shows the atomic percent (at. %) composition of the samples determined from XPS measurements (the XPS detection depth is only few nanometers). The composition of the samples is quite similar, although there is some C contamination on the samples surface (adventitious C and organic remnants from the electrolyte, in the form of C-C, C-O and C=O bonds), if one evaluates the F/Ti ratio, quite similar results are obtained.

The crystal structure of different morphologies of nanostructures was examined by XRD (see in **Fig 7**). For the same morphologies evaluated by XPS, we observe no difference in the XRD patterns; namely, layers are amorphous and there is no sign of crystallinity (no anatase peaks are detected, including the main peak ≈25.4°), for various water content in the electrolyte (6 or 8 M) and different applied voltages in the 10 to 58 V range, for anodization times of up to 2.5 h. We further investigated the influence of anodization time on crystallinity and we evaluated a nanoporous layer (diameter ≈13 nm) obtained in 5 h and by further increasing the anodization time to 24 h, the resulting nanotubular layer (diameter ≈20 nm). Interestingly, even though at 5 h we notice a very small anatase peaks (that can also be due to background noise), for the 24 h anodization we observe distinct anatase peaks: the main anatase peak at ≈25.4° and the lower intensities peak at ≈47.5° and ≈53.8°. So, for longer anodization times, the as-grown layer contains anatase crystals in the amorphous TiO_2 lattice, but the amorphous phase is not fully converted to a crystalline one.

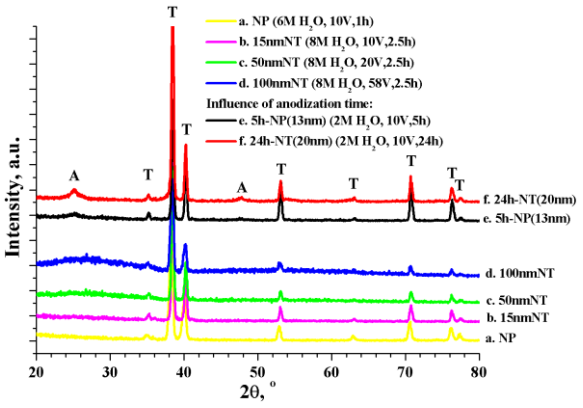

Fig. 7. XRD patterns of the selected nanostructures, nanopores and different diameter (15, 50 or 100 nm) nanotubes (a. to d.) and for nanostructures obtained at different anodization time, of 5h and 24h (e. and f., respectively).

Conclusion

The present work reports on the key factors influencing the morphology of self-organized TiO_2 nanostructures obtained by electrochemical anodization of Ti foils in HF containing EG based electrolytes. The resulting nanostructures, either nanopores or nanotubes, have an open top morphology with a hexagonal, uniform arrangement. Further investigations were performed for establishing the effect of water content in the electrolyte on the nanostructured surface morphology and the effects on the pore-wall-splitting mechanism converting nanopores to nanotubes. XPS measurement confirmed that there is no significant difference in the at % composition at the top of nanostructures, either nanopores or nanotubes. XRD patterns confirm the amorphous structure of the as-grown layers, however, for longer anodization times (e.g. 24 h) there is low crystallinity in the form of anantase phase. Improvement in the morphology and uniformity of TiO_2 nanostructures (nanopores or nanotubes of desired morphology) impacts their use for specific bioapplications, for which surface morphology sensitivity or high aspect ratio are required.

Acknowledgements

The authors would like to acknowledge Slovenian Research Agency (ARRS) grants No. P2-0232, P3-0388, J1-6728 for financial support. Ulrike Marten-Jahns is acknowledged for XRD measurements. DFG and Erlangen DFG cluster of excellence are acknowledged for financial support.

Author contributions

Conceived the plan: M. Kulkarni and A. Mazare together performed all experiments and data analysis. A. Iglic and P. Schmuki made guidance for experimental work and for writing. Authors have no competing financial interests.

Reference

1. Sul, Y. T.; Johansson, C. B.; Petronis, S.; Krozer, A.; Jeong, Y.; Wennerberg, A.; Alrbektsson, T.; *Biomaterials*, **2002,** *23*, 491. **DOI:** 10.1016/S0142-9612(01)00131-4
2. Yang, B.; Uchida, M.; Kim, H. M.; Zhan, X.; Kokubo, T.; *Biomaterials*, **2004,** *25*, 1003. **DOI:** 10.1016/S0142-9612(03)00626-4
3. Liu, X.; Chu, P.K.; Ding, C.; *Mater. Sci. Eng.*, **2004,** *R 47*, 49. **DOI:** 10.1016/j.mser.2004.11.001
4. Kumar, M.; Kumar, T.; Devesh Kumar, A.; *Scr.Mater*, **2014,** 105, 46. **DOI:** 10.1016/j.scriptamat.2015.04.030
5. Enachi, M.; Lupan, O.; Braniste, T.; Sarua, A.; Chow, L.; Mishra, Y. K.; Gedamu, D.; Adelung, R.; Tiginyanu, I.; *Phys. Status Solidi Rapid Res. Lett.*,**2015,** 9, 171. **DOI:** 10.1002/pssr.201570615
6. Assefpour-Dezfuly, M.; Vlachos, C.; Andrews, E. H.; *J. Mater. Sci.*, **1984**, *19* 3626. **DOI:** 10.1007/BF00552275
7. Zwilling, V.; Aucouturier, M.; Darque-Ceretti, E.; *Electrochim. Acta*, **1999**, *45*, 921. **DOI:** 10.1016/S0013-4686(99)00283-2
8. Zwilling, V.; Darque-Ceretti, E.; Boutry-Forveille, A.; David, D.; Perrin, M.Y.; Aucouturier, M.; *Surf. Interf. Anal.*, **1999,** *27*, 629. **DOI:** 10.1002/(SICI)1096-9918(199907)27:7
9. Tsai, C.C.; Teng, H.S.; *Chem. Mater.*, **2004**, *16*, 4352. **DOI:** 10.1021/cm049643u
10. Maiyalagan, T.; Viswanathan, B.; Varadarju, U.V.; *Bull. Mater. Sci.*, **2006**, *29*, 705. **DOI:** 10.1088/0957-4484/18/29/295604
11. M28: Hoyer, P.; *Langmuir*, **1996,** *12* 1411. **DOI:** 10.1021/la9507803
12. Kulkarni, M. et al; *Nanotechnology*, **2015,** *26*, 062002. **DOI:** 10.1088/0957-4484/26/6/062002
13. Lee, K.; Mazare, A.; Schmuki, P.; *Chem. Rev.*, 2014, 114, 9385. **DOI:** 10.1021/cr500061m
14. Hahn, R.; Schmuki, P.; Kirchgeorg, R.; ECS meeting abstracts, 2014, Abstract MA2014-02 1376.
15. Mor, G.K.; Varghese, O.K.; Paulose, M.; Shankar, K.; Grimes, C.A.; *Sol. Energy Mater. Sol. Cells*, **2006,** *90*, 2011. **DOI:** 10.1016/j.solmat.2006.04.007
16. Tsuchiya, H.; Macak, J.M.; Taveira, L.; Balaur, E.; Ghicov, A.; Sirotna, K.; Schmuki, P.; *Electrochem. Commun.*, **2005,** *7*, 576. **DOI:** 10.1016/j.elecom.2005.04.008
17. Ghicov, A.; Tsuchiya, H.; Macak, J.M.; Schmuki, P.; *Electrochem. Commun.*, **2005**, *7*, 505. **DOI:** 10.1016/j.elecom.2005.03.007
18. Macak, J.M.; Schmuki, P.; *Electrochim. Acta*, **2006**, *52*, 1258. **DOI:** 10.1016/j.electacta.2006.07.021
19. Macak, J.M.; Hildebrand, H.; Marten-Jahns, U.; Schmuki, P.; *J. Electroanal. Chem.*, **2008**, *621*, 254. **DOI:** 10.1016/j.jelechem.2008.01.005
20. Grigorescu, S.; Pruna, V.; Titorencu, I.; Jinga, V.V.; Mazare, A.; Schmuki, P.; Demetrescu, I.; *Bioelectrochem.*,**2014,** *98*, 39. **DOI:** 10.1016/j.bioelechem.2014.03.002
21. Mazare, A.; Ionita, D.; Totea, G.; Demetrescu, I.; *Surf. Coat. Technol.* **2014**, *252*, 87. **DOI:** 10.1016/j.surfcoat.2014.04.049
22. Naghizadeh, M.; Ghannadi1, S.; Abdizadeh, H.; Golobostanfard, M.R.; *Adv. Mat. Res.*, **2015.** **DOI:** 10.4028/www.scientific.net/AMR.829.907
23. M34: Geetha, M.; Singh, A.; Asokamani, R.; Gogia, A.; *Prog. Mater. Sci.*, **2009,** *54*, 397. **DOI:** 10.1016/j.pmatsci.2008.06.004
24. Kulkarni, M. et al.; Mazare, A.; Schmuki, P.; Iglič, A.; Nanomedicine (Manchester: One Central Press) **2013,** 111
25. Bauer, S.; Kleber, S.; Schmuki, P.; Electrochem. Commun., **2006,** *8*, 1321. **DOI:** 10.1016/j.elecom.2006.05.030
26. M6: Park, J.; Bauer, S.; von der Mark, K.; Schmuki, P.; *Nano Lett.*, **2007,** *7*, 6. **DOI:** 10.1021/nl070678d
27. Spatz, J. P.; Cell-Nanostructure Interactions. In *Nanobiotechnology*; Wiley-VCH Verlag: Weinheim, Germany, **2004**; pp 53-65.
28. Wagner, V.; Dullaart, A.; Bock, A. K.; Zweck, A.; *Nat. Biotechnol.* **2006,** 24, 1211. **DOI:** 10.1038/nbt1006-1211
29. M36: Bauer, S.; Park, J.; Faltenbacher, J.; Berger, S.; von der Mark, K.; Schmuki, P.; *Integr. Biol.*, **2009,** *1*, 525. **DOI:** 10.1039/B908196H
30. Bauer, S.; Park, J.; Pittrof, A.; Song, Y.; von der Mark, K.; Schmuki, P.; *Integr. Biol.*, **2011,** *3*, 927. **DOI:** 10.1039/c0ib00155d
31. Park, J.; Bauer, S.; Pittrof, A.; Killian, M. S.; Schmuki, P.; von der Mark, K.; *Small*, **2012**, *8*, 98. **DOI:** 10.1002/smll.201100790
32. Park, J.; Bauer, S.; Schlegel, K.A.; Neukam, F.W.; von der Mark, K.; Schmuki, P.; *Small*, **2009,** *5*, 666. **DOI:** 10.1002/smll.200801476
33. Ercan, B.; Taylor1, E.; Alpaslan, E.; Webster, T.J.; *Nanotechnology*, **2011,** *22*, 295102. **DOI:** 10.1088/0957-4484/22/29/295102
34. Smith, B.S.; Capellato, P.; Kelley, S.; Gonzalez-Juarrero, M.; Popat, K.C.; *Biomater. Sci.*, **2013,** *1*, 322. **DOI:** 10.1039/C2BM00079B
35. Neacsu, P.; Mazare, A.; Cimpean, A.; Park, J.; Costache, M.; Schmuki, P.; Demetrescu, I.; *Int. J. Biochem. Cell Biol.*, **2014**, *55*, 187. **DOI:** 10.1016/j.biocel.2014.09.006
36. Neacsu, P.; Mazare, A.; Schmuki, P.; Cimpean, A.; *Int. J. Nanomed.*, **2015.**
37. Bauer, S.; Park, J.; Pittrof, A.; von der Mark, K.; Schmuki, P.; *Biomed Tech.*,**2012**, *08*, 57(SI-1 Track-G). **DOI:** 10.1515/bmt-2012-4015
38. Monteiro, D. R.; Gorup, L. F.; Takamiya, A. S.; Ruvollo-Filho, A. C.; de Camargo, E. R.; Barbosa, D. B.; *Int. J. Antimicrob. Agents*, **2009,** *34*, 103. **DOI:** 10.1016/j.ijantimicag.2009.01.017
39. Zhao, L.; Wang, H.; Huo, K.; Cui, L.; Zhang, W.; Ni, H.; Zhang, Y.; Wu, Z.; Chu, P. K.; *Biomaterials*, **2011,** *32* 5706. **DOI:** 10.1016/j.biomaterials.2011.04.040.
40. Mazare, A.; Totea, G.; Burnei, C.; Schmuki, P.; Demetrescu, I.; Ionita, D.; *Corro. Sci.*, **2015.**
41. Mazare, A.; Dilea, M.; Ionita, D.; Titorencu, I.; Trusca, V.; Vasile, E.; *Bioelectrochem.*, **2012,** *87*, 124. **DOI:** 10.1016/j.bioelechem.2012.01.002
42. M11: Valota, A.; LeClere, D.J.; Skeldon, P.; Curioni, M.; Hashimoto, T.; Berger, S.; Kunze, J.; Schmuki, P.; Thompson, G.E.; *Electrochim Acta*, **2009**, *54*, 4321. **DOI:** 10.1016/j.electacta.2009.02.098
43. Nishanthi, S.T.; Iyyapushpam, S.; Padiyan, D.P.; *IEEE*, **2013,** 3, 978-1-4799-1379-4/13 **DOI:** 10.1109/ICANMEET.2013.6609302
44. Ali, G.; Chen, C.; Yoo, S.H.; Kum, J.M.; Cho, S.O.; *Nanoscale Res. Lett.*, **2011**, *6*, 332 **DOI:** 10.1186/1556-276X-6-332
45. Wei, W.; Berger, S.; Hauser, C.; Meyer, K.; Yang, M.; Schmuki, P.; *Electrochem. Commun*, **2010,** *12*, 1184. **DOI:** 10.1016/j.elecom.2010.06.014

